Supporting Information

Reactivity of Ketenyl Anions towards Ammonia

Prakash Duari, [a] Mike Jörges ,[a] Sunita Mondal,[a] Kai-Stephan Feichtner[a] and Viktoria H. Gessner *[a]

[a]Faculty of Chemistry and Biochemistry, Ruhr-University Bochum, 44801 Bochum, Germany, Email: viktoria.gessner@rub.de

Table of Contents

The original files to all analysis methods have been uploaded to an online repository and can be downloaded via the following link. Sole exceptions are the data of the single-crystal X-ray diffraction experiments. Cif files have been deposited with the CCDC (see chapter 4 for details).

Link to data repository: https://doi.org/10.17877/RESOLV-2025-MIIS9122

1. Experimental Procedures

1.1. General Information

Chemical and Conditions

If not stated otherwise, all experiments were carried out using standard Schlenk techniques under an argon atmosphere, which was dry and free of oxygen. Argon (99.999%) was a product of *Air Liquide* and was used without any further drying. An MBraun SPS 800 was used to dry solvents before their usage (THF, toluene, DCM, ACN, *n*-pentane, *n*-hexane). All solvents were stored over molecular sieves under an argon atmosphere. Reagents were purchased from Sigma-Aldrich, ABCR, Acros Organics or TCI Chemicals and used without further purification if not stated otherwise. $\mathbf{1}^{\mathbf{CN}}$, $\mathbf{1}^{\mathbf{Tos}}$, $\mathbf{1}^{\mathbf{PS}}$, $\mathbf{1}^{\mathbf{PSe}}$ were synthesized following literature procedures.[1-4] The formation of $\mathbf{2}^{\mathbf{CN}}$ has been reported previously by our group.[2]

Analytical methods

NMR Spectroscopy. ^{1}H, $^{13}C\{^{1}H\}$, $^{77}Se\{^{1}H\}$, $^{31}P\{^{1}H\}$ NMR spectra were recorded on Avance-III-400 spectrometers at 22 °C if not stated otherwise. All values of the chemical shift are in ppm regarding the δ-scale. All spin-spin coupling constants (*J*) are printed in Hertz (Hz). To display multiplicities and signal forms correctly the following abbreviations were used: s = singlet, d = doublet, t = triplet m = multiplet, dd = doublet of doublet, br = broad signal. Signal assignment was supported by, HSQC (^{1}H / ^{13}C), HMBC (^{1}H / ^{13}C, ^{1}H / ^{31}P) correlation experiments.

IR spectra were recorded on a Shimadzu IRSpirit with QATR-S module in an argon filled glovebox and on a Thermo Nicolet iS5 FT-IR in transmission mode with a Specac “Omni-cell” with KBr plates and a 0.1 mm spacer at 22 °C. Measurement and processing details for individual spectra can be extracted from the corresponding tables in the supporting information.

Melting points were measured with the SMP30 melting point apparatus from Stuart.

Elemental analyses were performed on an Elementar vario MICRO cube elemental analyzer.

For details about the single-crystal Xray diffraction analyses, see chapter 3.

Safety comments

Caution! Strong bases such as alkali metal bases, especially as neat compounds, are severely air-/moisture-sensitive and pyrophoric organometallic compounds. These compounds need to be handled under an inert gas atmosphere to exclude reactions with oxygen and water. Guidelines for their handling can be found in literature: T. L. Rathman, J. A. Schwindeman, *Org. Process Res. Dev.* **2014**, *18*, 1192.

Caution! Ammonia (NH_3). This should not be added while the reaction mixture is still frozen to prevent overpressure inside the system. Removing the gases from the reaction should be done by purging the reaction vessel with Argon or N_2 inside a ventilated fume hood.

Caution! Carbon monoxide (CO) is a highly toxic gas and should be handled only in a well-ventilated fume hood, with a CO detector next to the reaction setup.

1.2. Synthesis of compounds 2^{Tos}

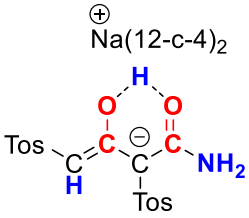

50 mg (0.088 mmol) $\mathbf{1}^{Tos}$ was dissolved in 2 mL DCM inside a *J*-Young NMR tube. The solution was frozen, and the atmosphere in the tube was replaced with NH_3. The NMR tube was shaken overnight. After that, the solvent was removed to obtain a white solid. After extraction with 2 mL THF, followed by vapor diffusion with diethyl ether, $\mathbf{2}^{Tos}$ was obtained as a white solid (15 mg, 0.019 mmol, 44%).

^{1}H-NMR (400 MHz, THF-d_8): δ = 7.72 and 7.71 (d, 2H+2H, $^3J_{HH}$ = 8.1 Hz; $^3J_{HH}$ = 8.0 Hz, C$H_{Tos,o}$), 7.20 (d, 2H, $^3J_{HH}$ = 8.1 Hz, C$H_{Tos,m}$), 7.16 (d, 2H, $^3J_{HH}$ = 8.0 Hz, C$H_{Tos,m}$), 4.47 (s, 1H, Tos-C*H*=C), 3.62 (s, 32H +residual crown, C$H_{2,crown}$,), 2.37 (s, 3H, C$H_{3,Tos}$), 2.34 (s, 3H, C$H_{3,Tos}$) ppm. The peaks for the NH_2 groups and the bridging proton could not be observed. The assignment of the signal to the Tos-C*H*=C group is confirmed by 2D-^{1}H-^{13}C correlation experiments. **^{13}C{^{1}H}-NMR** (101 MHz, THF-d_8): δ = 172.1 (s, *C*=O), 144.7 (s, $C_{Tos,p}$), 143.8 (s, $C_{Tos,p}$), 141.9 (s, $C_{Tos,ipso}$), 139.5 (s, $C_{Tos,ipso}$),129.6 (s, C$H_{Tos,m}$), 129.6 (s, C$H_{Tos,m}$), 129.5 (s, C$H_{Tos,o}$), 127.3 (s, C$H_{Tos,o}$), 113.0 (s, C-$C^{(-)}$-C(O)NH_2), 85.2 (s, Tos-*C*H=C), 71.4 (s, $CH_{2,crown}$), 21.7 (s, $CH_{3,Tos}$), 21.6 (s, $CH_{3,Tos}$) ppm. **FT-IR** (ATR, cm^{-1}): 2981.4 (w), 2962.7 (w), 2868.4 (w), 1652.9 (m), 1597.7 (m), 1447.6 (w), 1365.0 (m), 1301.1 (m), 1135.2 (s), 1095.0 (m), 1021.8 (s), 916.2 (s), 850.2 (m), 812.8 (m), 659.2 (w), 644.1 (s), 540.7 (w), 512.7 (s), 483.3 (w). Attempts to obtain satisfactory elemental analysis data were repeatedly unsuccessful.

$\mathbf{2}^{Tos}$ exists predominantly as the enol tautomer, as evidenced by NMR spectroscopy. In contrast, the corresponding cyano derivative was found to adopt the β-ketoamide form. The preference for different tautomers may arise from subtle electronic differences imparted by the cyano and tosyl substituents. However, we cannot exclude that cation–anion interactions may also contribute to this behaviour.

1.3. Synthesis of compounds 3^{PS}

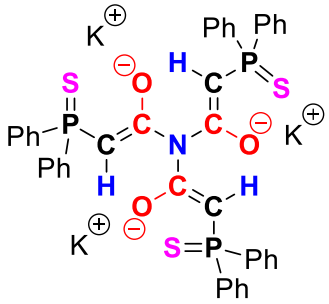

300 mg (1.01 mmol) of compound $\mathbf{1}^{PS}$ was dissolved in 10 mL THF. The solution was frozen, and the atmosphere in the flask was replaced with NH_3. The solution was then stirred for 3 days. Afterward, by slow vapor diffusion of hexane into the saturated solution, compound $\mathbf{3}^{PS}$ could be obtained as a slightly yellow crystalline product (257 mg, 0.284 mmol, 85 %). Single-crystal X-ray diffraction analysis was performed on those crystals.

^{1}H-NMR (400 MHz, THF-d_8): δ = 8.05 – 7.95 (m, 6H, C$H_{Ph,ortho}$), 7.93 – 7.85 (m, 6H, C$H_{Ph,ortho}$), 7.39 – 7.30 (m, 9H, C$H_{Ph,meta,para}$), 7.11 – 7.02 (m, 3H, C$H_{Ph,para}$), 6.87 – 6.78 (m, 6H, C$H_{Ph,meta}$), 4.03j (d, $^2J_{HP}$ = 25.7, 3H, PC*H*CO), 3.64 – 3.60 (m, C$H_{2,THF}$), 1.82 – 1.75 (m, C$H_{2,THF}$) ppm. **^{13}C{^{1}H}-NMR** (101 MHz, THF-d_8): δ = 173.2 (d, $^2J_{CP}$ = 9.1 Hz, PCH*C*O), 140.9 (d, $^1J_{CP}$ = 85.8 Hz, $CH_{Ph,ipso}$), 139.9 (d, $^1J_{CP}$ = 82.4 Hz, $CH_{Ph,ipso}$), 132.8 (d, $^3J_{CP}$ = 11.2 Hz, $CH_{Ph,ortho}$), 132.1 (d, $^3J_{CP}$ = 9.9 Hz, $CH_{Ph,ortho}$), 130.3 (s, $CH_{Ph,para}$), 129.7 (s, $CH_{Ph,para}$), 128.5 (d, $^4J_{CP}$ = 11.6 Hz, $CH_{Ph,meta}$), 128.2 (d, $^4J_{CP}$ = 12.3 Hz, $CH_{Ph,meta}$), 68.4 (s, $CH_{2,THF}$), 63.8 (d, $^1J_{CP}$ = 110.9 Hz, P*C*HCO), 26.6 (s, $CH_{2,THF}$) ppm. **^{31}P{^{1}H}-NMR** (162 MHz, THF-d_8): δ = 32.38 (s, PPh_2S) ppm. **FT-IR** (ATR, cm^{-1}): 3050.4 (w), 2935.5 (w), 2873.04 (w),1574.8 (w), 1550.3 (s), 1495.8 (s), 1435.4 (s), 1153.9 (m), 1066.4 (m), 1027.6 (m), 998.8 (w), 860.3 (s), 789.9 (m), 741.8 (s), 700.8 (m), 692.9 (m), 623.3 (s), 603.2 (s), 507.7 (s), 483.3 (w). **Anal. Calcd** for

$C_{54}H_{57}K_3NO_6P_3S_3$: C, 57.78; H, 5.12; N, 1.25; S, 8.57. Found: C, 57.51; H, 4.92; N, 1.30; S, 8.78.

1.4. Synthesis of compounds 2^{PSe}

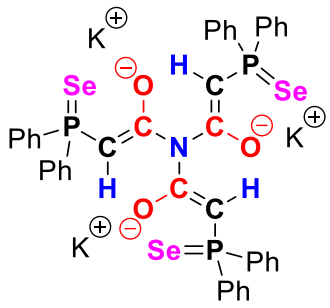

120 mg (0.350 mmol) of compound $\mathbf{1}^{PSe}$ was dissolved in 5 mL THF. The atmosphere of the flask was replaced by NH_3 gas. The solution was stirred for 3 days at room temperature. Vapor diffusion of hexane to the reaction mixture, resulting in the colorless crystals of $\mathbf{3}^{PSe}$, which were filtered off and dried in vacuo after washing with diethyl ether. (100 mg, 0.0955 mmol, 83%). Single-crystal X-ray diffraction analysis was performed on those crystals.

^{1}H-NMR (400 MHz, THF-d_8): δ = 8.02 – 7.93 (m, 6H, C*H*$_{Ph,ortho}$), 7.90 – 7.84 (m, 6H, C*H*$_{Ph,ortho}$), 7.39 – 7.32 (m, 9H, C*H*$_{Ph,meta,para}$), 7.13 – 7.07 (m, 3H, C*H*$_{Ph,para}$), 6.89 – 6.82 (m, 6H, C*H*$_{Ph,meta}$), 4.09 (d, $^2J_{HP}$ = 25.0 Hz, 3H, PC*H*CO) ppm. **^{13}C{^{1}H}-NMR** (101 MHz, THF-d_8): δ = 173.3 (d, $^2J_{CP}$ = 9.2 Hz, PCH*C*O), 139.6 (d, $^1J_{CP}$ = 77.3 Hz, *C*H$_{Ph,ipso}$), 138.6 (d, $^1J_{CP}$ = 77.3 Hz, *C*H$_{Ph,ipso}$), 133.0 (d, $^3J_{CP}$ = 11.2 Hz, *C*H$_{Ph,ortho}$), 132.6 (d, $^3J_{CP}$ = 10.2 Hz, *C*H$_{Ph,ortho}$), 130.5 (s, *C*H$_{Ph,para}$), 129.9 (s, *C*H$_{Ph,para}$), 128.6 (d, $^4J_{CP}$ = 11.8 Hz, *C*H$_{Ph,meta}$), 128.2 (d, $^4J_{CP}$ = 12.8 Hz, *C*H$_{Ph,meta}$), 63.1 (d, $^1J_{CP}$ = 102.4 Hz, P*C*HCO). **^{31}P{^{1}H}-NMR** (162 MHz, THF-d_8): δ = 19.14 (s, *P*Ph$_2$Se) ppm. **^{77}Se-NMR** (76 MHz, THF-d_8): δ = –236.3 and –236.6 (d, $^1J_{PSe}$ = 641.9 and 639.2 Hz, PPh$_2$*Se*) ppm. **FT-IR** (ATR, cm^{-1}): 3051.0 (w), 2076.6 (w), 1669.5 (w), 1554.6 (m), 1479.2 (w), 1434.7 (s), 1382.3 (m), 1346.4 (m), 1156.1 (w), 1095.8 (s), 998.1 (w), 847.3 (m), 741.0 (s), 522.7 (w). Attempts to obtain satisfactory elemental analysis data were repeatedly unsuccessful.

1.5. Synthesis of compounds 4^{PS}

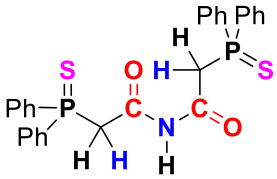

30 mg (0.0267 mmol) of compound $\mathbf{3}^{PS}$ was dissolved in 2 mL THF. An excess amount of H_2O was added to that solution and stirred for 30 min. The resulting solution was filtered. Vapor diffusion of hexane to the reaction mixture, resulting in the colorless crystals of $\mathbf{4}^{PS}$, which were filtered off and dried in *vacuo*. (11 mg, 0.0206 mmol, 77%). Single-crystal X-ray diffraction analysis was performed on those crystals.

^{1}H-NMR (400 MHz, THF-d_8): δ = 9.79 (s, 1H, N*H*), 7.87 – 7.78 (m, 8H, C*H*$_{Ph,ortho}$), 7.62 – 7.46 (m, 6H, C*H*$_{Ph,meta,para}$), 3.83 (d, $^2J_{HP}$ = 25.0 Hz, 4H, PC*H*$_2$CO) ppm. **^{13}C{^{1}H}-NMR** (101 MHz, THF-d_8): δ = 164.6 (d, $^2J_{CP}$ = 5.1 Hz, PCH$_2$*C*O), 132.5 (d, $^4J_{CP}$ = 3.1 Hz, *C*H$_{Ph,para}$), 131.9 (d, $^1J_{CP}$ = 84.2 Hz, *C*H$_{Ph,ipso}$), 131.6 (d, $^2J_{CP}$ = 11.0 Hz, *C*H$_{Ph,ortho}$), 129.2 (d, $^3J_{CP}$ = 12.6 Hz, *C*H$_{Ph,meta}$), 43.6 (d, $^1J_{CP}$ = 44.9 Hz, P*C*H$_2$CO) ppm. **^{31}P{^{1}H}-NMR** (162 MHz, THF-d_8): δ = 37.08 ppm. **FT-IR** (ATR, cm^{-1}): 3263.7(w), 3008.8 (w), 2909.7 (w), 1749.2 (m), 1733.45 (m), 1676.7 (m), 1585.5 (w), 1576.2 (m), 1495.8 (m), 1482.8 (s), 1401.7 (s), 1302.6 (s), 1161.8 (w), 1100.8 (s), 998.1 (m), 774.6 (s) 603.9 (s), 542.1 (m), 519.9 (s), 417.9 (s). **Anal. Calcd** for $C_{28}H_{25}NO_2P_2S_2$: C, 63.03; H, 4.72; N, 2.62; S, 12.02. Found: C, 63.13; H, 5.08; N, 2.54; S, 12.02.

2. Proposed mechanistic pathways to 2 and 3

Initially we hypothesized that the divergent reactivity of ketenyl anions **1**^{CN} and **1**^{Tos}, leading to the β-ketoamides **2** instead of **3**, arises from their lower basicity due to the stronger electron-withdrawing ability of the tosyl and cyano group. We assumed that, in contrast to the triamide formation, the reaction to **2** is initiated by nucleophilic attack of ammonia at the ketenyl C2 carbon atom. However, attempts to optimize the structure of the putative NH3 adduct resulted in spontaneous ammonia elimination suggesting that the ketenyl anion cannot act as electrophile and that the selectivity is instead governed by steric effects. We therefore propose that both reactions are initiated by deprotonation of NH_3. While the resulting ketene readily reacts with another equivalent of the ketenyl anions **1**^{CN} or **1**^{Tos}, it preferentially reacts with the less nucleophilic NH_2- rather than with the sterically more demanding ketenyl anions **1**^{PS} and **1P**^{Se}, leading to triamide **3** instead of **2** (Figure S1).

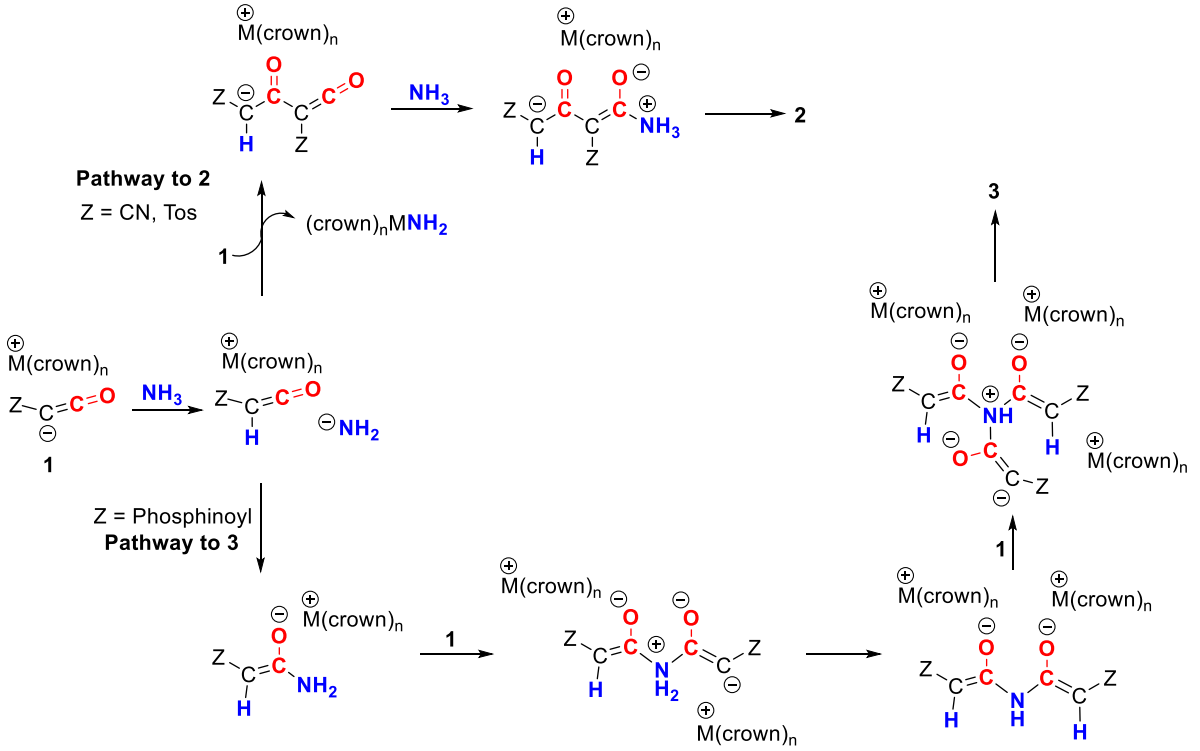

Figure S1. Proposed reaction mechanisms for **2** and **3**.

The formation of **2** and **3** is proposed to proceed via an initial proton transfer from NH_3 to the ketenyl anion, yielding the neutral ketene Z(H)C=C=O. In the pathway leading to **2**, a second equivalent of the ketenyl anion nucleophilically attacks the C=O moiety of the ketene, accompanied by elimination of $(crown)_nMNH_2$. Subsequently, a second ammonia molecule nucleophilically attacks at the C2 carbon of the ketene moiety furnish **2** after tautomerization.

For the pathway to **3**, the amide anion attacks the C=O bond of the neutral ketene to afford an anionic amide, which again nucleophilically attacks the second, and then third molecule of ketenyl anion in a stepwise manner. This pathway may also proceed via deprotonation of the anionic amide by the ketenyl anion and subsequent attach of the dianion at the neutral ketene. This pathway is favoured for phosphinoyl-substituted ketenyl anions, presumably due to their greater steric demand which slows down nucleophilic attack of the ketenyl anion compared to the attack of amide NH_2^-.

3. NMR and IR Spectra of the isolated compounds

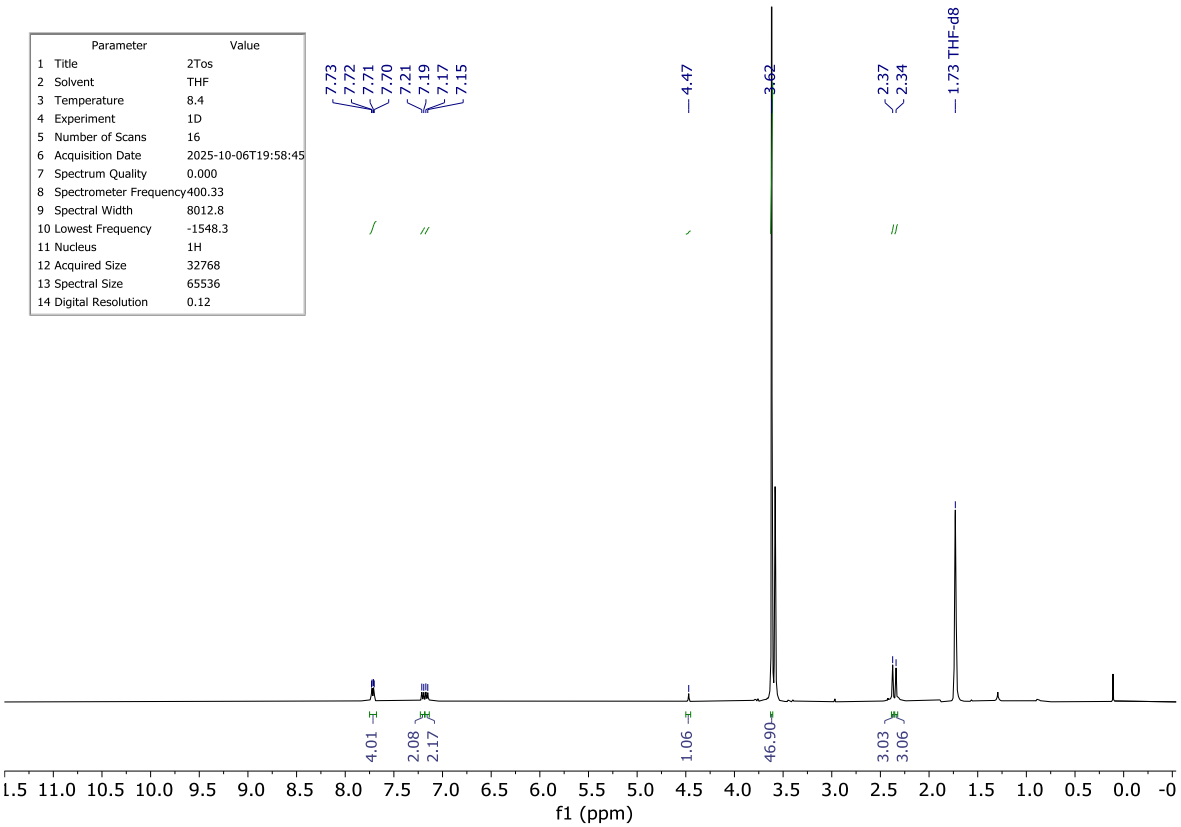

Figure S 2 ^{1}H NMR spectrum of compound **2^{Tos}** in THF-d_8.

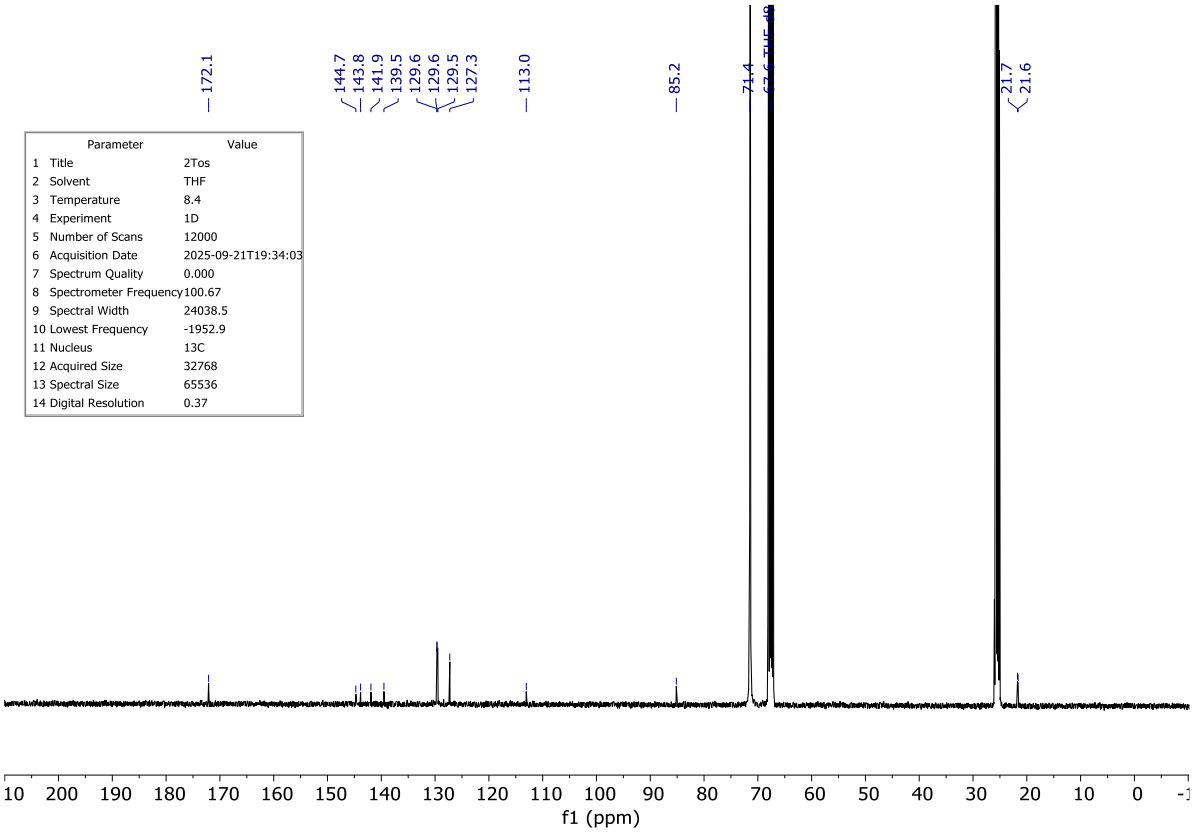

Figure S3 ^{13}C{^{1}H} NMR spectrum of compound **2^{Tos}** in THF-d_8.

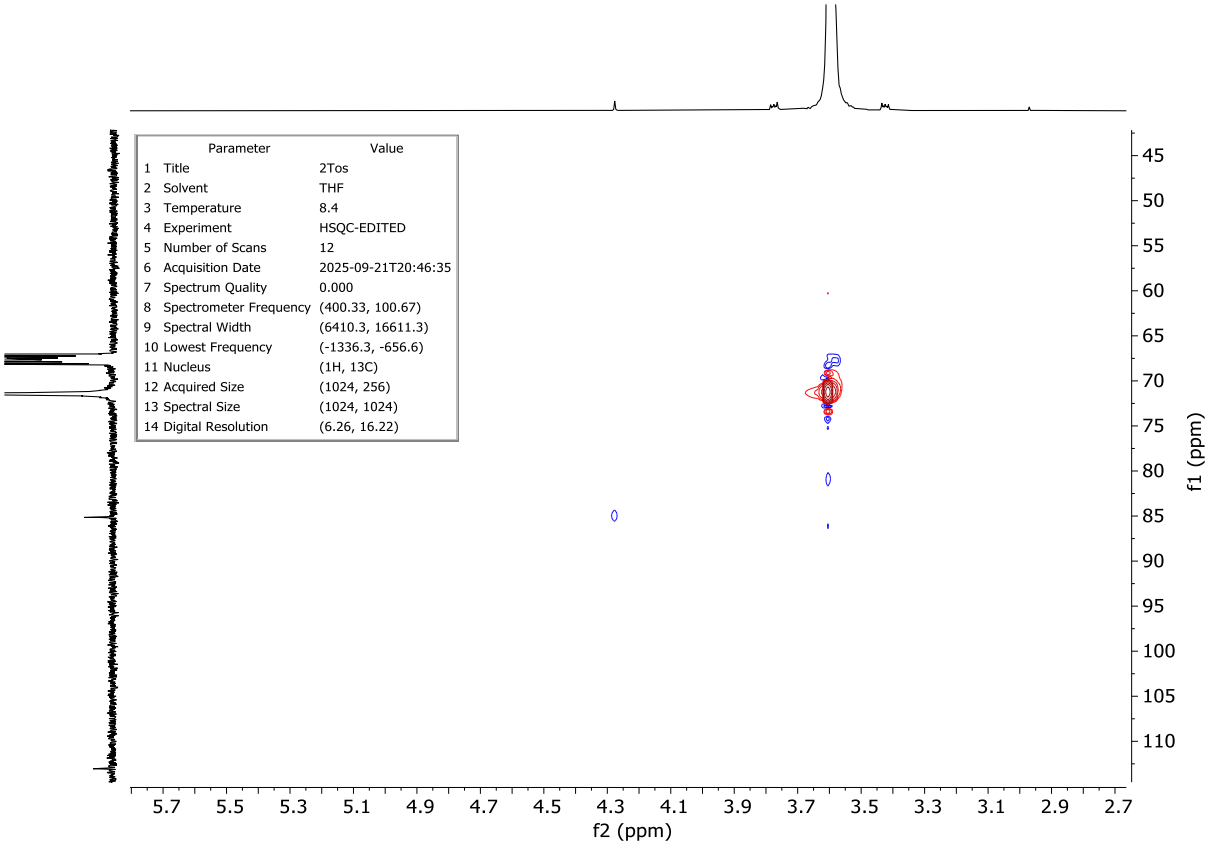

Figure S4 ^{1}H-$^{13}C\{^{1}H\}$-HSQC spectrum of **2^{Tos}** in THF-d_8.

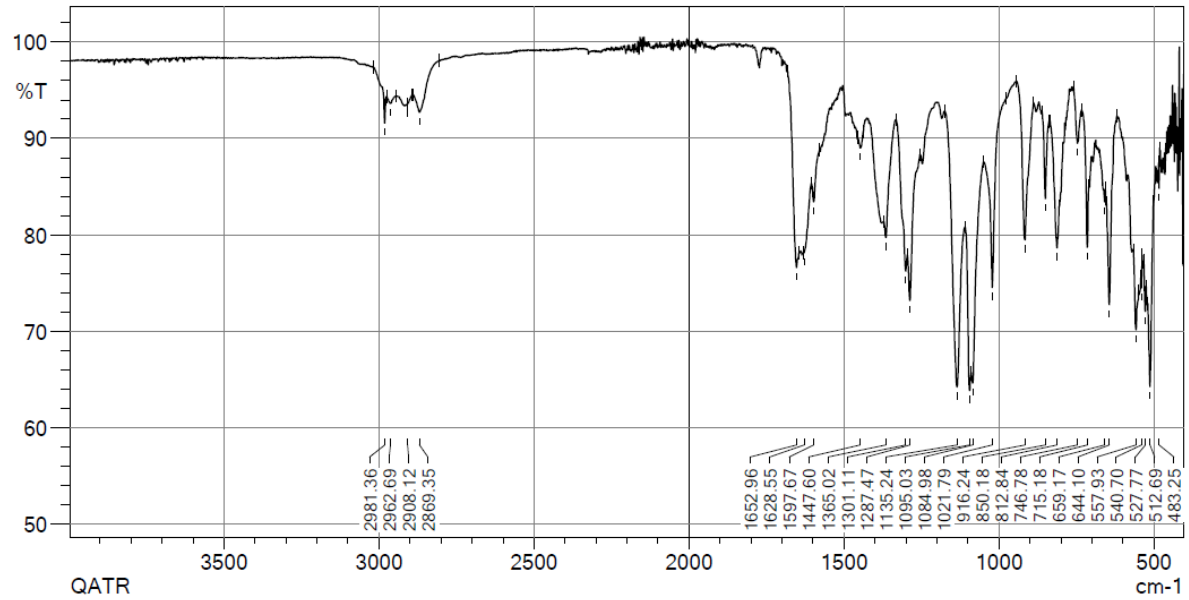

Figure S5 IR spectrum of compound **2^{Tos}** (solid state).

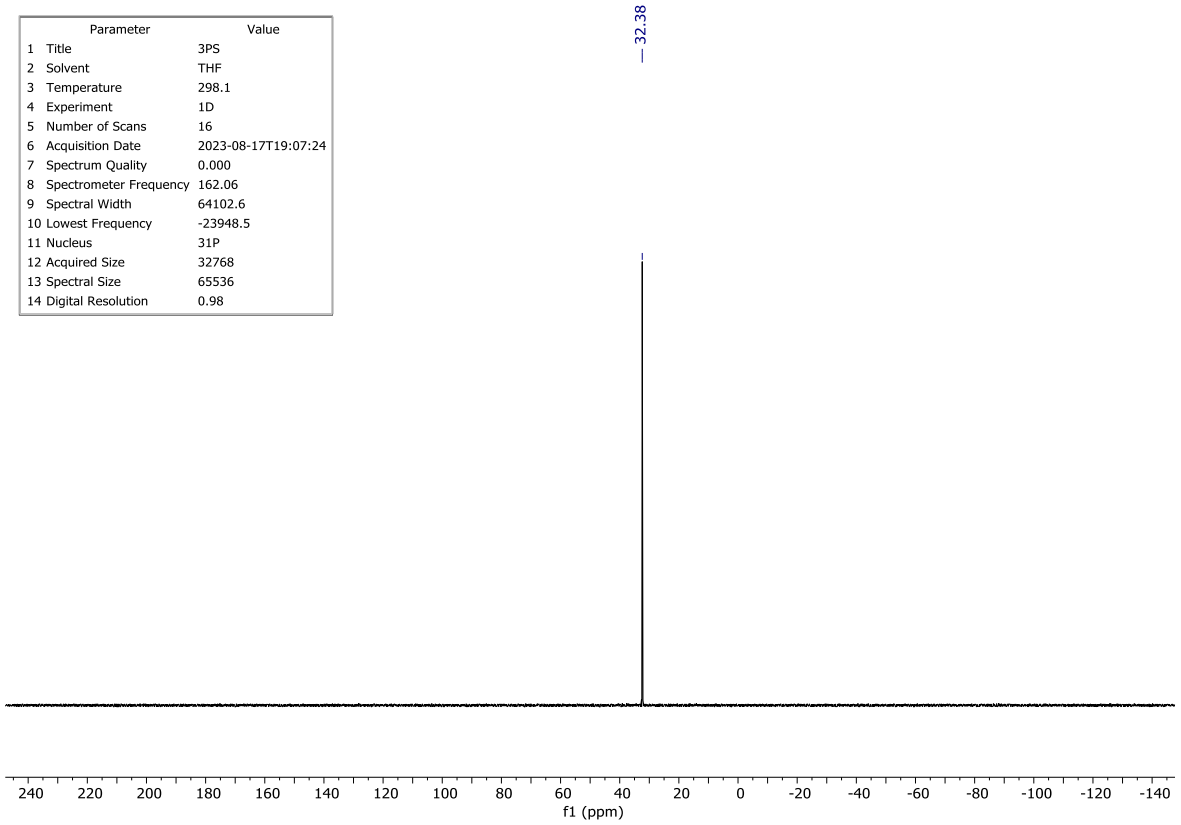

Figure S6 $^{31}P\{^{1}H\}$ NMR spectrum of compound **3^{PS}** in THF-d_8.

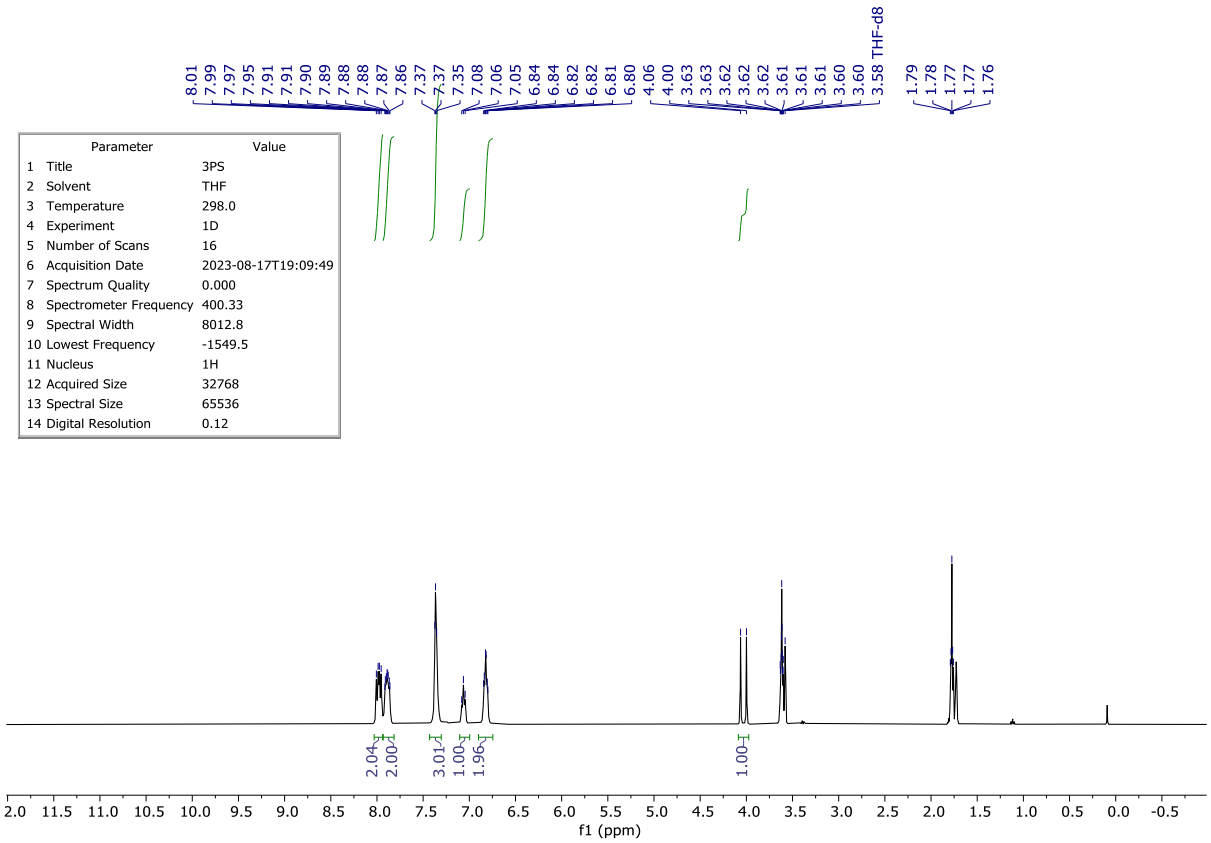

Figure S7 ^{1}H NMR spectrum of compound **3^{PS}** in THF-d_8.

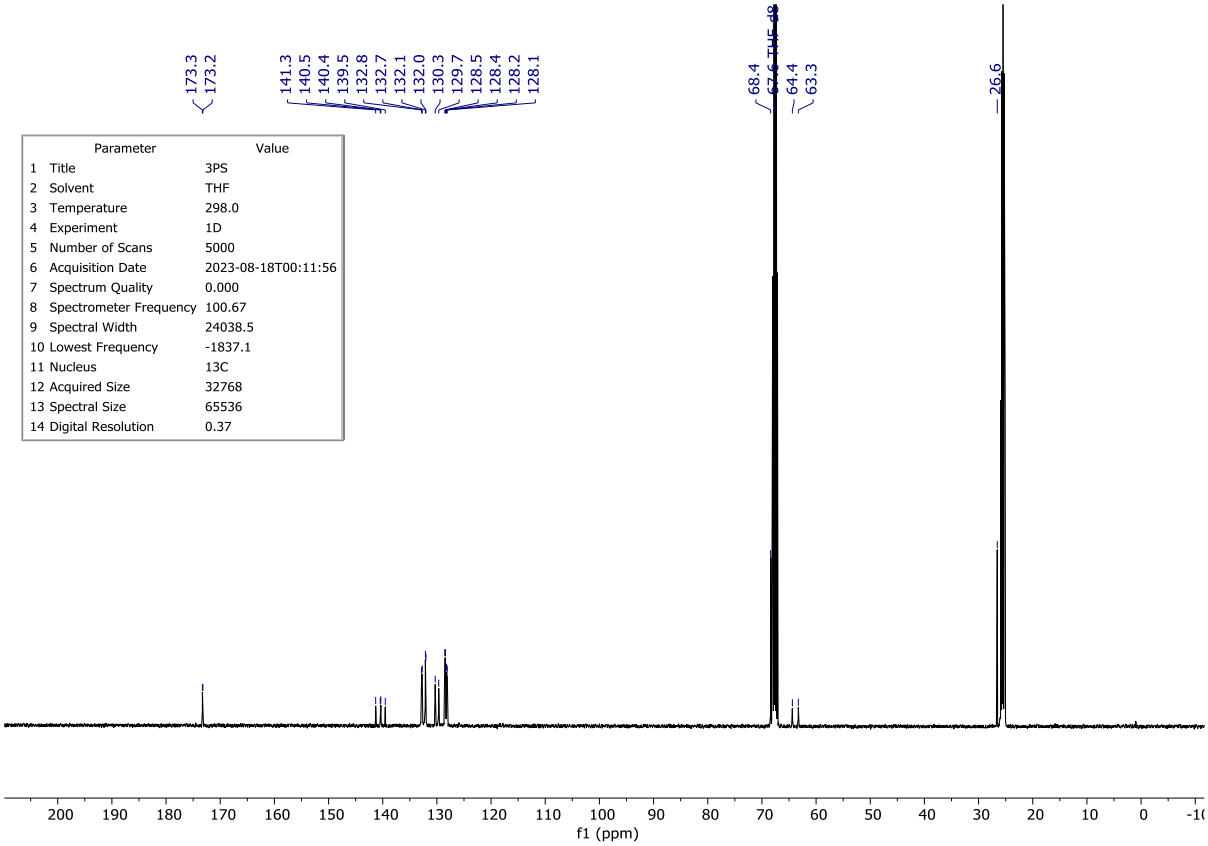

Parameter	Value
1 Title	3PS
2 Solvent	THF
3 Temperature	298.0
4 Experiment	1D
5 Number of Scans	5000
6 Acquisition Date	2023-08-18T00:11:56
7 Spectrum Quality	0.000
8 Spectrometer Frequency	100.67
9 Spectral Width	24038.5
10 Lowest Frequency	-1837.1
11 Nucleus	13C
12 Acquired Size	32768
13 Spectral Size	65536
14 Digital Resolution	0.37

Figure S8 $^{13}C\{^{1}H\}$ NMR spectrum of compound **3^{PS}** in THF-d_8.

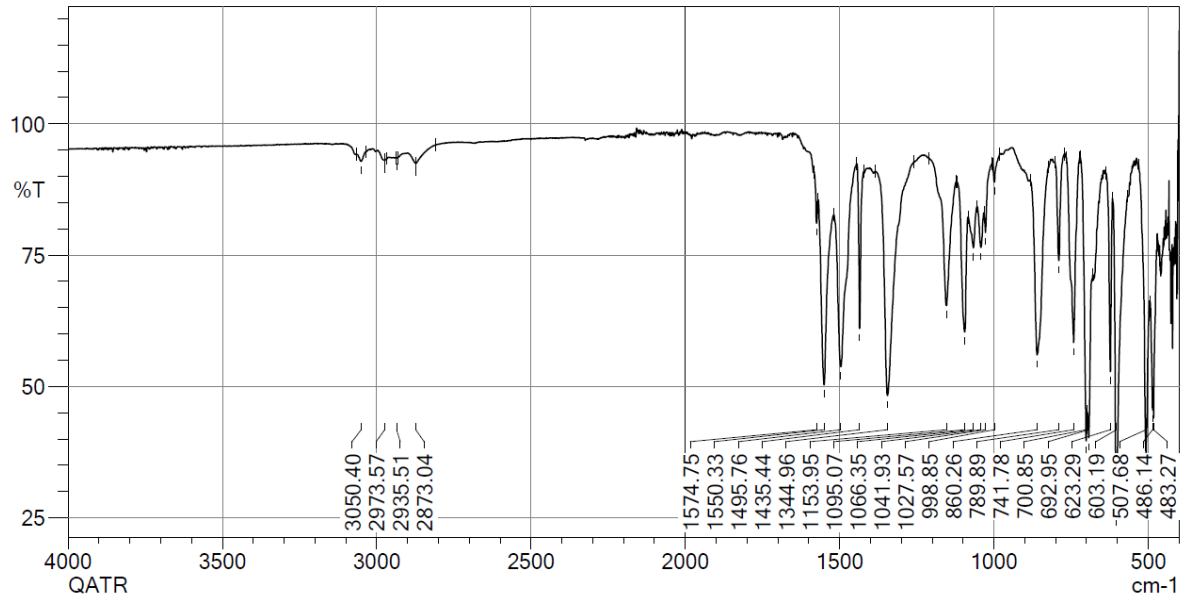

Figure S9 IR spectrum of compound **3^{PS}** (solid state).

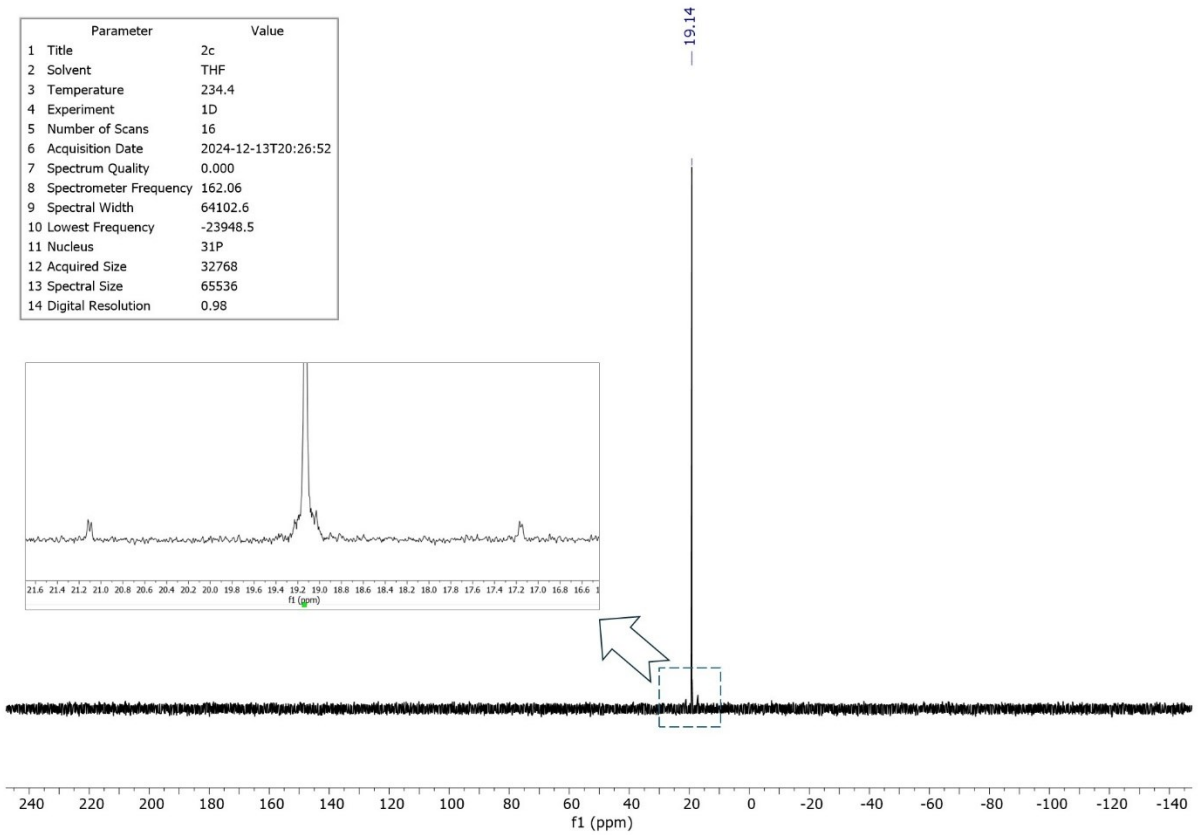

Figure S10 $^{31}P\{^{1}H\}$ NMR spectrum of compound **3^{PSe}** in THF-d_8 with showing the two selenium satellite peaks.

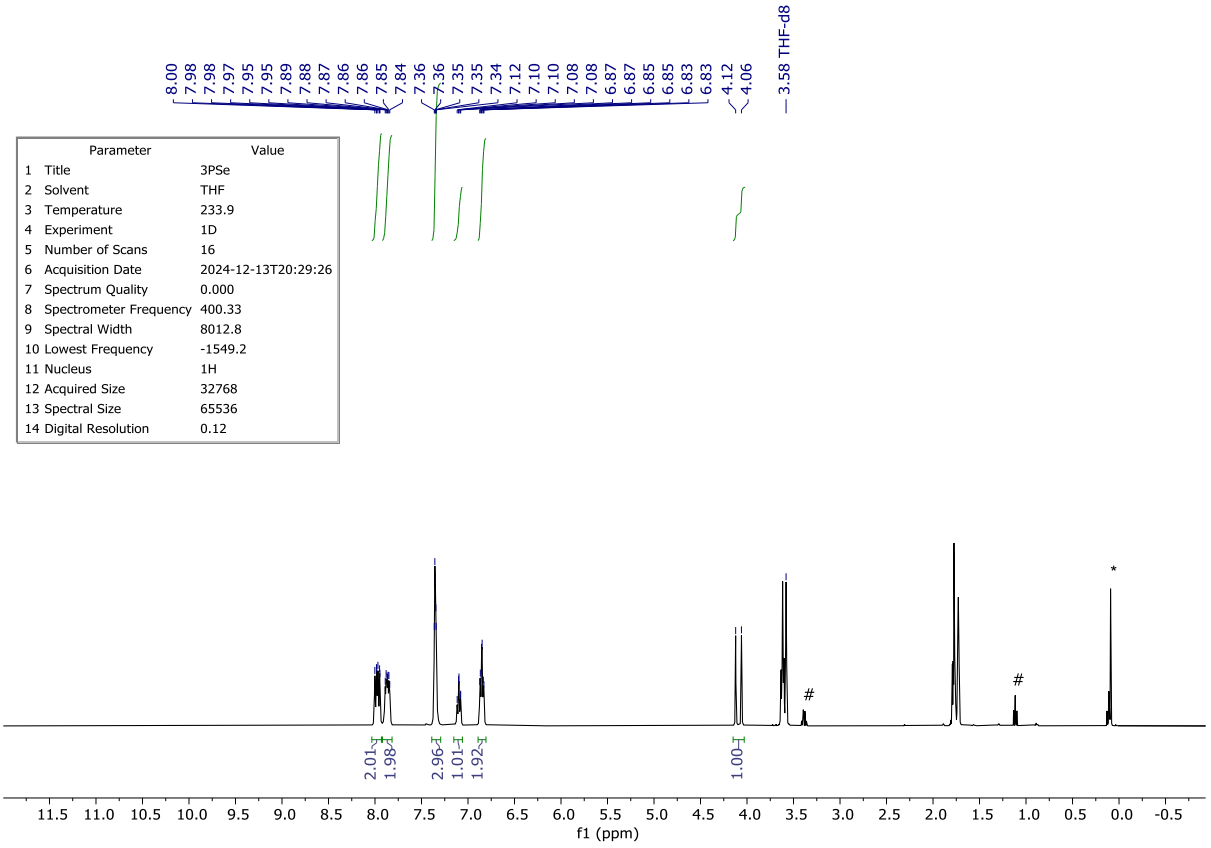

Figure S11 ^{1}H NMR spectrum of compound **3^{PSe}** in THF-d_8. # corresponds to signals of diethyl ether. * corresponds to silicon grease.

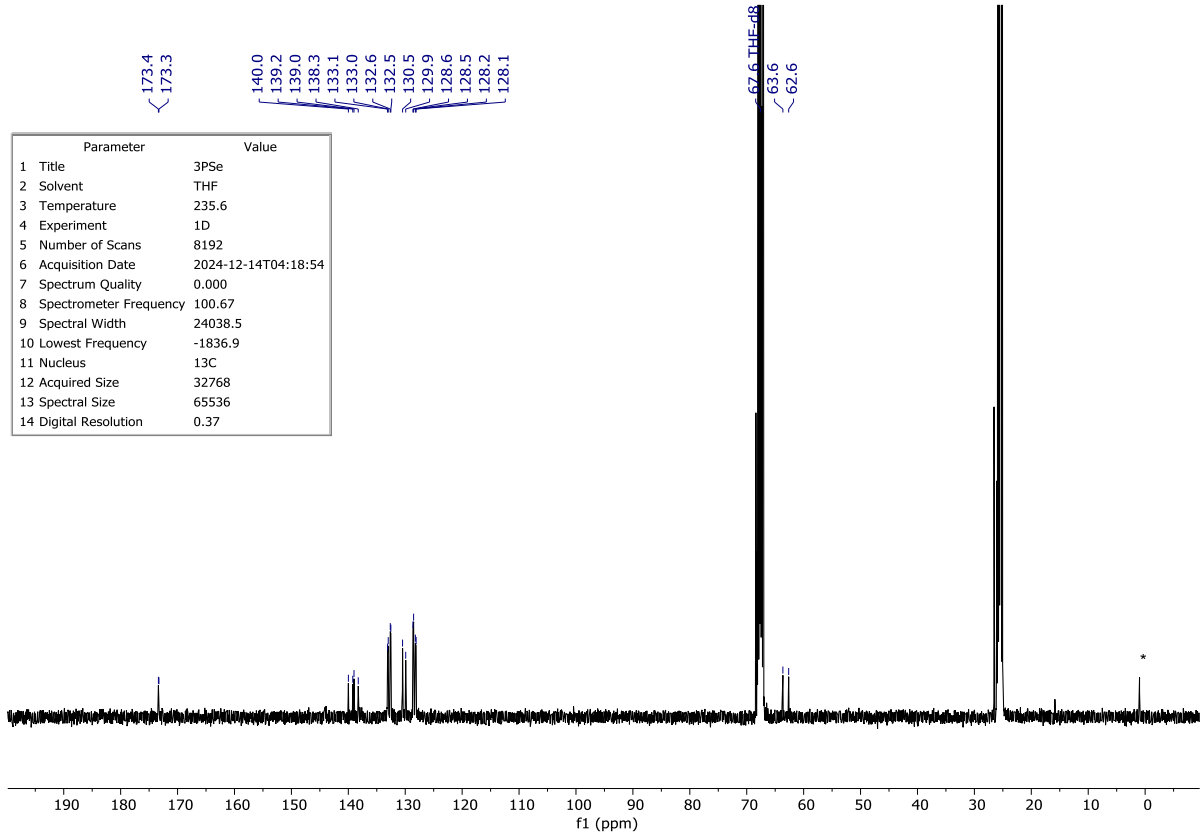

	Parameter	Value
1	Title	3PSe
2	Solvent	THF
3	Temperature	235.6
4	Experiment	1D
5	Number of Scans	8192
6	Acquisition Date	2024-12-14T04:18:54
7	Spectrum Quality	0.000
8	Spectrometer Frequency	100.67
9	Spectral Width	24038.5
10	Lowest Frequency	-1836.9
11	Nucleus	13C
12	Acquired Size	32768
13	Spectral Size	65536
14	Digital Resolution	0.37

Figure S12 $^{13}C\{^{1}H\}$ NMR spectrum of compound **3^{PSe}** in THF-d_8.

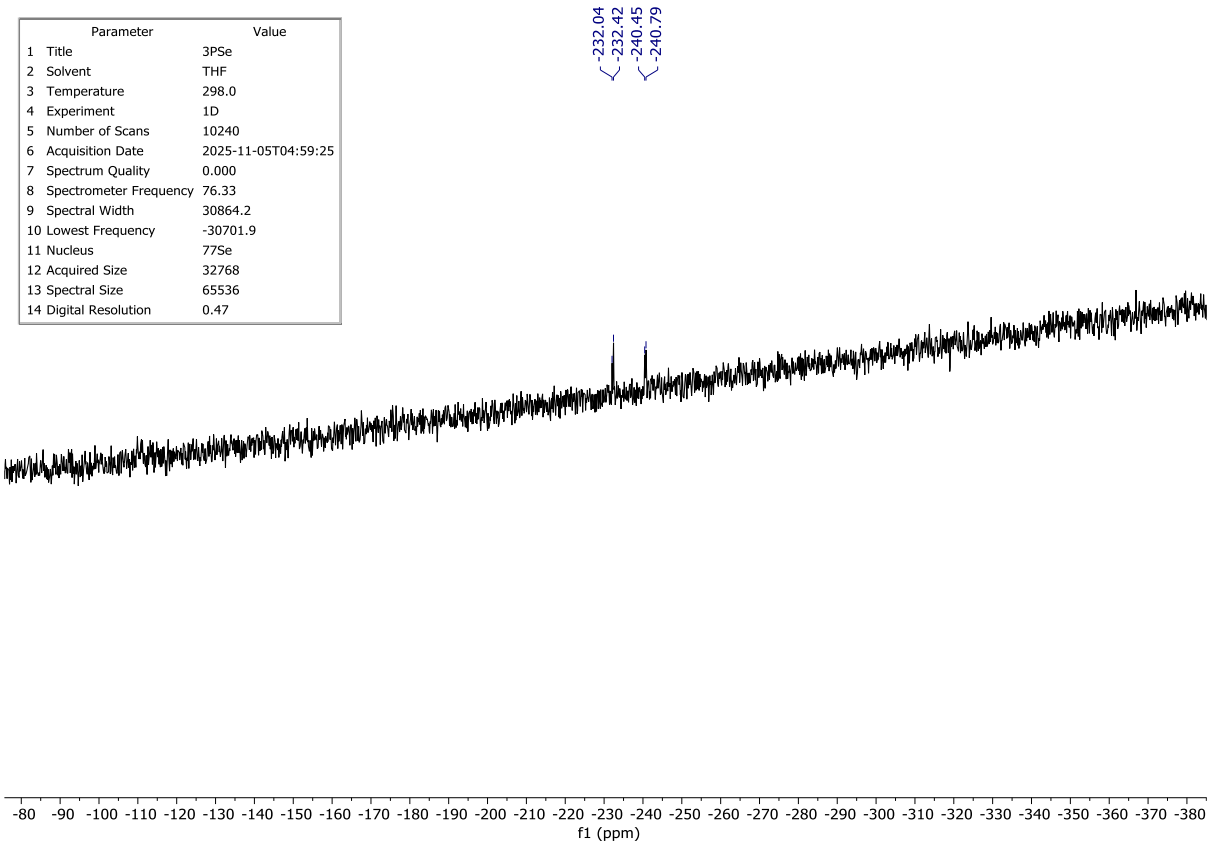

	Parameter	Value
1	Title	3PSe
2	Solvent	THF
3	Temperature	298.0
4	Experiment	1D
5	Number of Scans	10240
6	Acquisition Date	2025-11-05T04:59:25
7	Spectrum Quality	0.000
8	Spectrometer Frequency	76.33
9	Spectral Width	30864.2
10	Lowest Frequency	-30701.9
11	Nucleus	77Se
12	Acquired Size	32768
13	Spectral Size	65536
14	Digital Resolution	0.47

Figure S13 ^{77}Se NMR spectrum of compound **3^{PSe}** in THF-d_8.

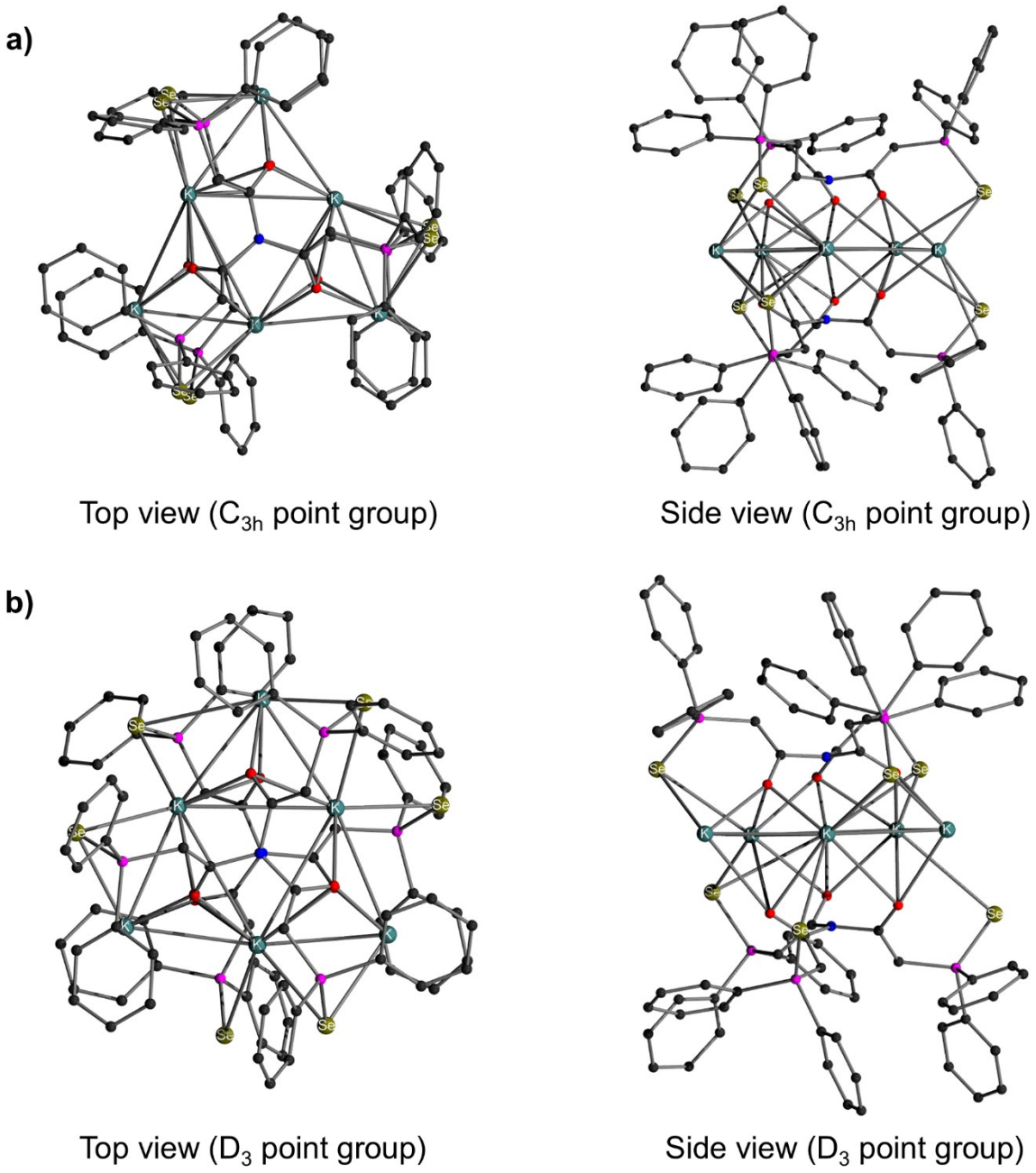

Figure S14. Display of the possible isomers of **3**^{PSe}. a) Representation of the C_{3h} point group (eclipsed configuration), which was also observed in the solid-state structure of compound **3**^{PSe}. b) Representation of the D_3 point group (staggered configuration). Note: These structures are non-optimized and are only shown to explain two peaks in the ^{77}Se NMR spectrum at room temperature.

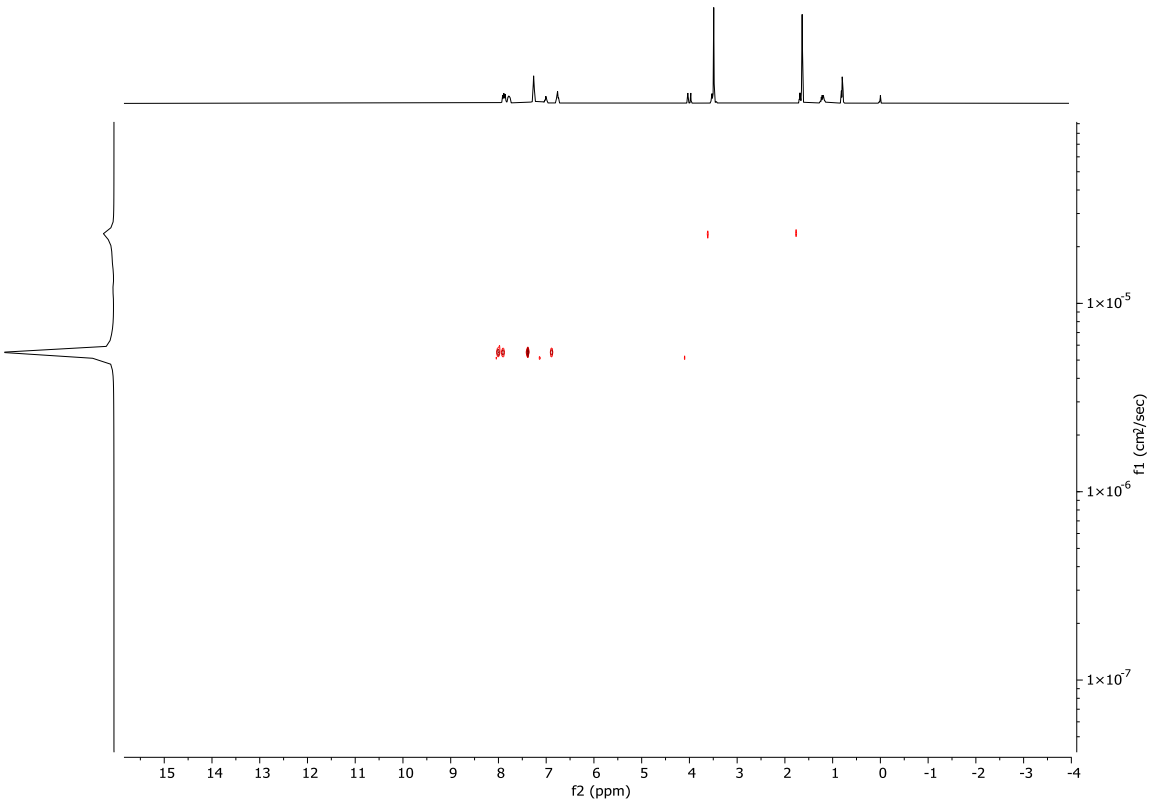

Figure S15. ^{1}H-DOSY NMR spectrum of compound **3^{PSe}** in C_6D_6 with chemical shifts (ppm) on the f2 axis and diffusion coefficients (cm^2 /sec) on the f1 axis. DOSY spectrum produced via MestreNova software with Bayesian method (Resolution factor: 1; Repetitions: 0).

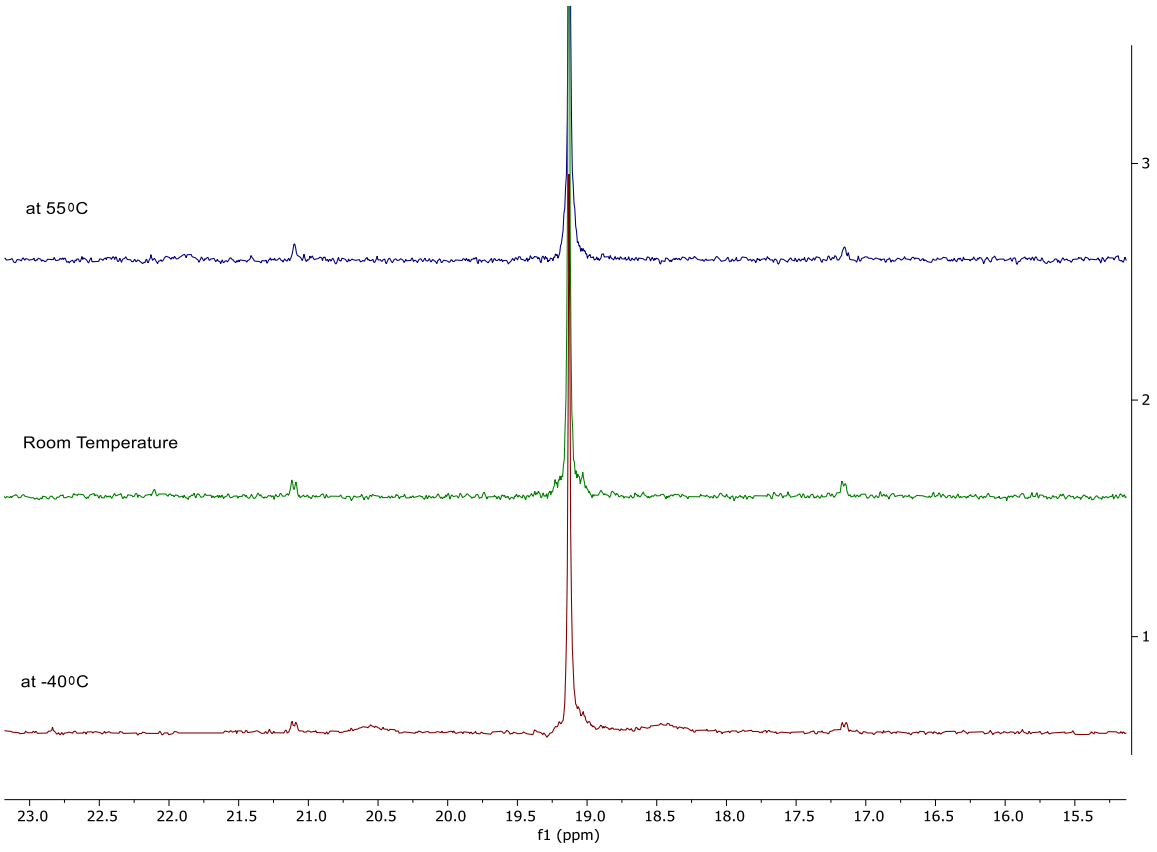

Figure S16. Stacked ^{31}P{^{1}H} NMR spectrum of compound **3^{PSe}** in THF-d_8 at 55 °C, room temperature and –40 °C. Note: at 55 °C the two satellite peaks for Se in both side of phosphorus peaks merge to a single peak.

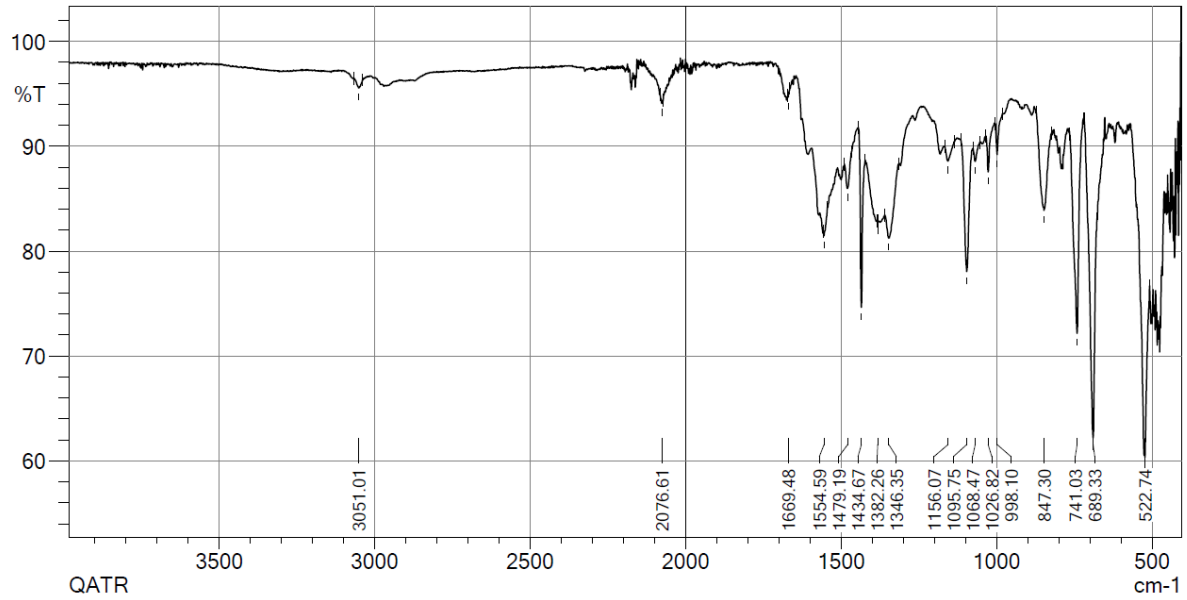

Figure S17. IR spectrum of compound $\mathbf{3^{PSe}}$ (solid state).

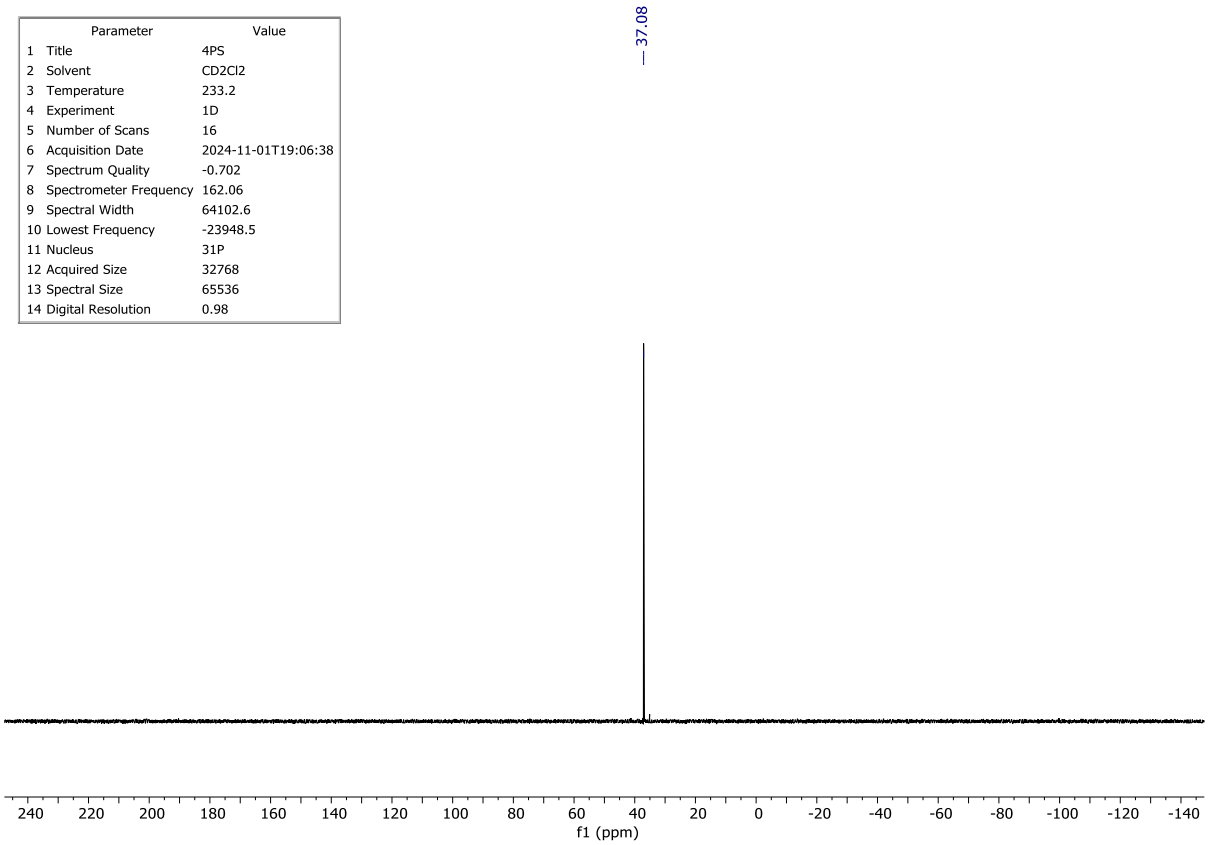

Figure S18. $^{31}P\{^{1}H\}$ NMR spectrum of compound $\mathbf{4^{PS}}$ in CD_2Cl_2.

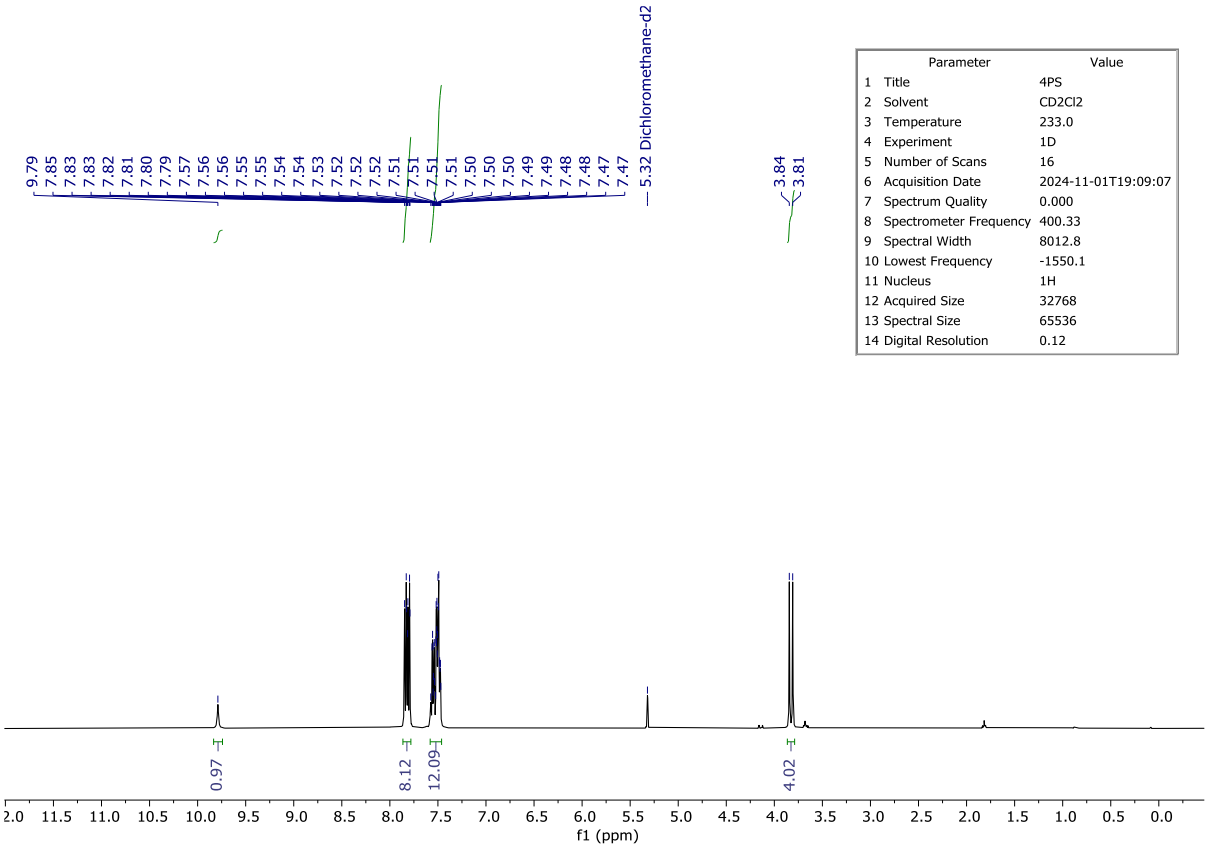

Parameter	Value
1 Title	4PS
2 Solvent	CD2Cl2
3 Temperature	233.0
4 Experiment	1D
5 Number of Scans	16
6 Acquisition Date	2024-11-01T19:09:07
7 Spectrum Quality	0.000
8 Spectrometer Frequency	400.33
9 Spectral Width	8012.8
10 Lowest Frequency	-1550.1
11 Nucleus	1H
12 Acquired Size	32768
13 Spectral Size	65536
14 Digital Resolution	0.12

Figure S19. ^{1}H NMR spectrum of compound **4^{PS}** in CD_2Cl_2.

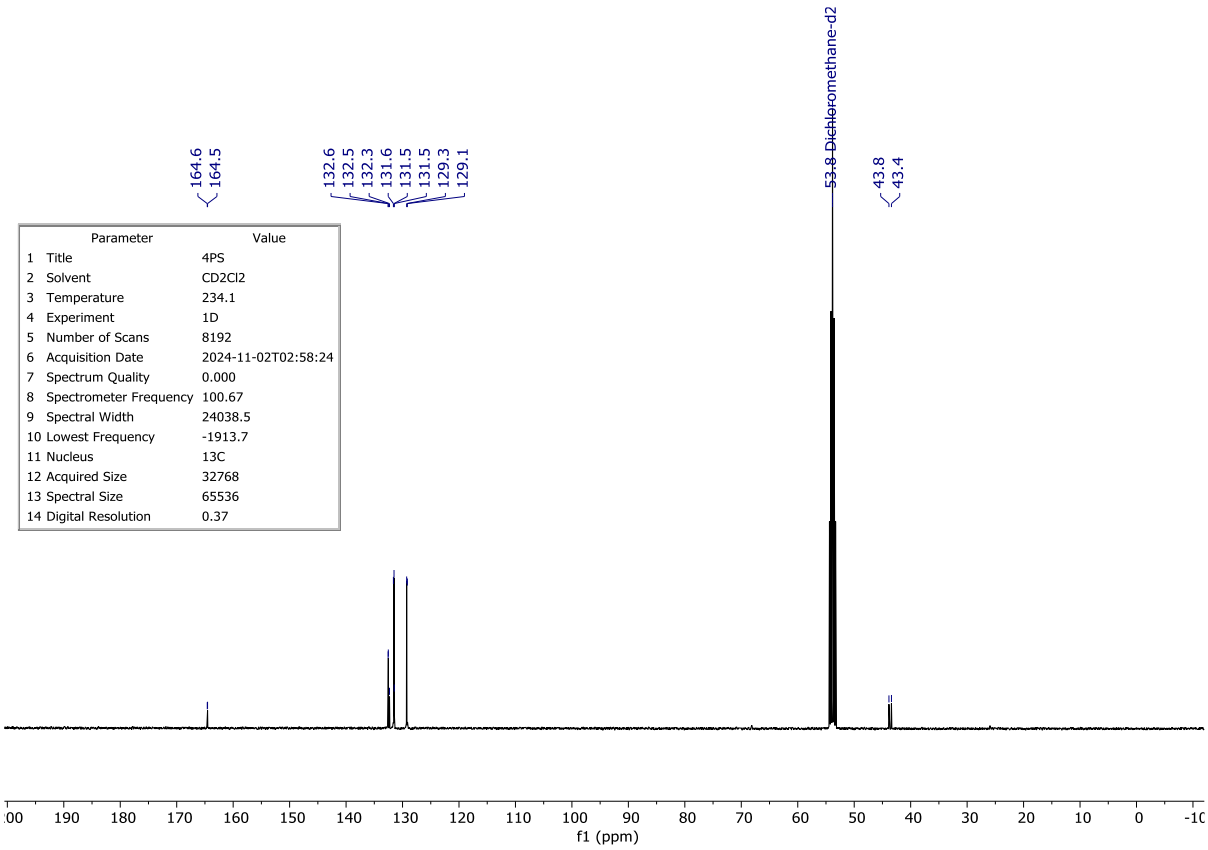

Parameter	Value
1 Title	4PS
2 Solvent	CD2Cl2
3 Temperature	234.1
4 Experiment	1D
5 Number of Scans	8192
6 Acquisition Date	2024-11-02T02:58:24
7 Spectrum Quality	0.000
8 Spectrometer Frequency	100.67
9 Spectral Width	24038.5
10 Lowest Frequency	-1913.7
11 Nucleus	13C
12 Acquired Size	32768
13 Spectral Size	65536
14 Digital Resolution	0.37

Figure S20. $^{13}C\{^{1}H\}$ NMR spectrum of compound **4^{PS}** in CD_2Cl_2.

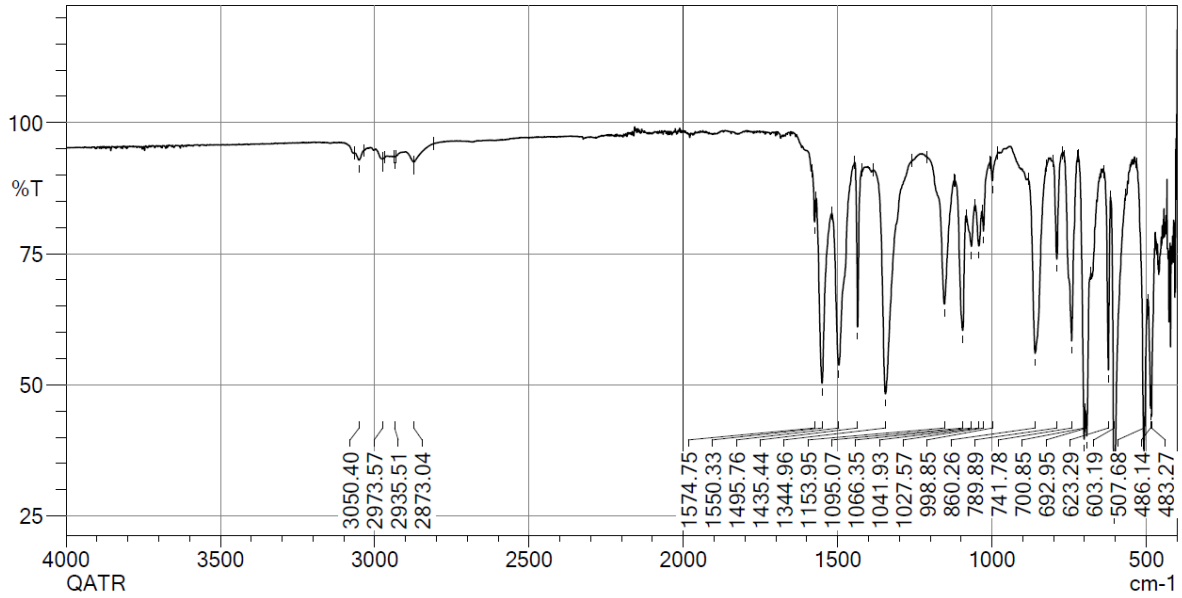

Figure S21. IR spectrum of compound **4**^{PS} (solid state).

4. Crystal structure determination

4.1. General information

High-quality single crystals of appropriate dimensions were placed in an inert oil such as perfluoropolyalkylether, hand-picked under polarized optical microscopy and then mounted on the diffractometer. The data collection was done at 100 K. X-ray intensity data measurements of all compounds were carried out on an Oxford SuperNova diffractometer with graphite-monochromatized (CuK_α= 1.54184 Å) radiation. The X-ray generator was operated at 50 kV and 30 mA.

All structures were solved by intrinsic phasing and refined by the full-matrix least-squares on F2 using software package and expanded using Fourier techniques.[5-8] Non-hydrogen atoms were refined anisotropically, while all hydrogen atoms were placed on the ideal positions using riding models and refined isotropically with displacement parameters constrained to those of the parent atoms (1.5 times Ueq for methyl groups and 1.2 times Ueq for all other carbon bound H).

Data collection and structure refinement details for all compounds are given in the following tables. Further details on the structure refinement are provided in the following sections for each individual structure.

Crystallographic data including structure factors have been deposited with the Cambridge Crystallographic Data Centre as supplementary publication no. CCDC - to CCDC - 2505654 Copies of the data can be gained free of charge on application to Cambridge Crystallographic Data Centre, 12 Union Road, Cambridge CB2 1EZ, UK; [fax: (+44) 1223-336-033; email: deposit@ccdc.cam.ac.uk].

Table S1. Data collection and structure refinement details for compounds **2b** and **2c.**

Compound	**3^{PS}**	**3^{PSe}**	**4^{PS}**
Formula	$C_{40}H_{60}KN_2O_{10}P$	$C_{116}H_{130}K_6N_2O_{14}P_6Se_6$	$C_{28}H_{25}NO_2P_2S_2$
CCDC	2505654	2505653	2505652
Formula weight	2244.79	2670.39	533.55
Temperature [K]	100(2)	100(2)	100(2)
Wave lenght [Å]	1.54184	1.54184	1.54184
Crystal system	Monoclinic	Monoclinic	Monoclinic
Space group	*Cc*	*P21/n*	*P21/n*
a [Å]	24.33755(12)	27.5782(2)	13.0525(2)
b [Å]	22.84495(10)	14.67560(10)	9.02100(10)
c [Å]	23.04768(11)	31.7159(2)	22.2487(3)
α[°]	90	90	90
β [°]	98.1107(4)	113.1020(10)	101.1780(10)
γ [°]	90	90	90
Volumen [$Å^3$]	12686.10(10)	11806.90(16)	2570.01(6)
Z	4	4	4
Calc. density [$Mg \cdot m^{-3}$]	1.175	1.502	1.379
μ ($Mo_{K\alpha}$) [mm^{-1}]	3.887	5.346	3.271
F(000)	4688	5440	1112
Crystal dimensions [mm]	0.193 x 0.153 x 0.088	0.150 x 0.090 x 0.080	0.110 x 0.080 x 0.060
Theta range θ [°]	2.665 to 67.075	2.841 to 67.999	3.648 to 76.821
Index ranges	-26<=h<=28	-30<=h<=33	-16<=h<=16
	-27<=k<=27,	-16<=k<=17	-10 <= k< = 11
	-27<=l<=27	-37<=l<=38	-28<=l<=26
Reflections collected	189911	159656	31399
Independent reflections	22119 [R(int) = 0.0443]	21491 [R(int) = 0.0677]	5290 [Rint = 0.0548]
Data/Restraints/Parameter	22119 / 168 / 1354	21491 / 762 / 1535	5290 / 0 / 316
Goodness-of-fit on F^2	1.038	1.127	1.050
Final R indices [I>2sigma(I)]	R1 = 0.0400, wR2 = 0.1069	R1 = 0.0551, wR2 = 0.1328	R1 = 0.0396, wR2 = 0.1087
Largest diff. peak and hole [e·Å-3]	0.304 and -0.328	1.328 and -0.683	0.647 and -0.412

4.2. Molecular structure of 3^{PS}

All hydrogen atoms were placed on ideal positions. The crystal structure contained two disordered THF molecules. The disorders were modelled using SADI, SIMU, and DELU restraints and refined using the PART instructions and free variables, which were optimized to occupancies of 65% and 35%; 29% and 71%.

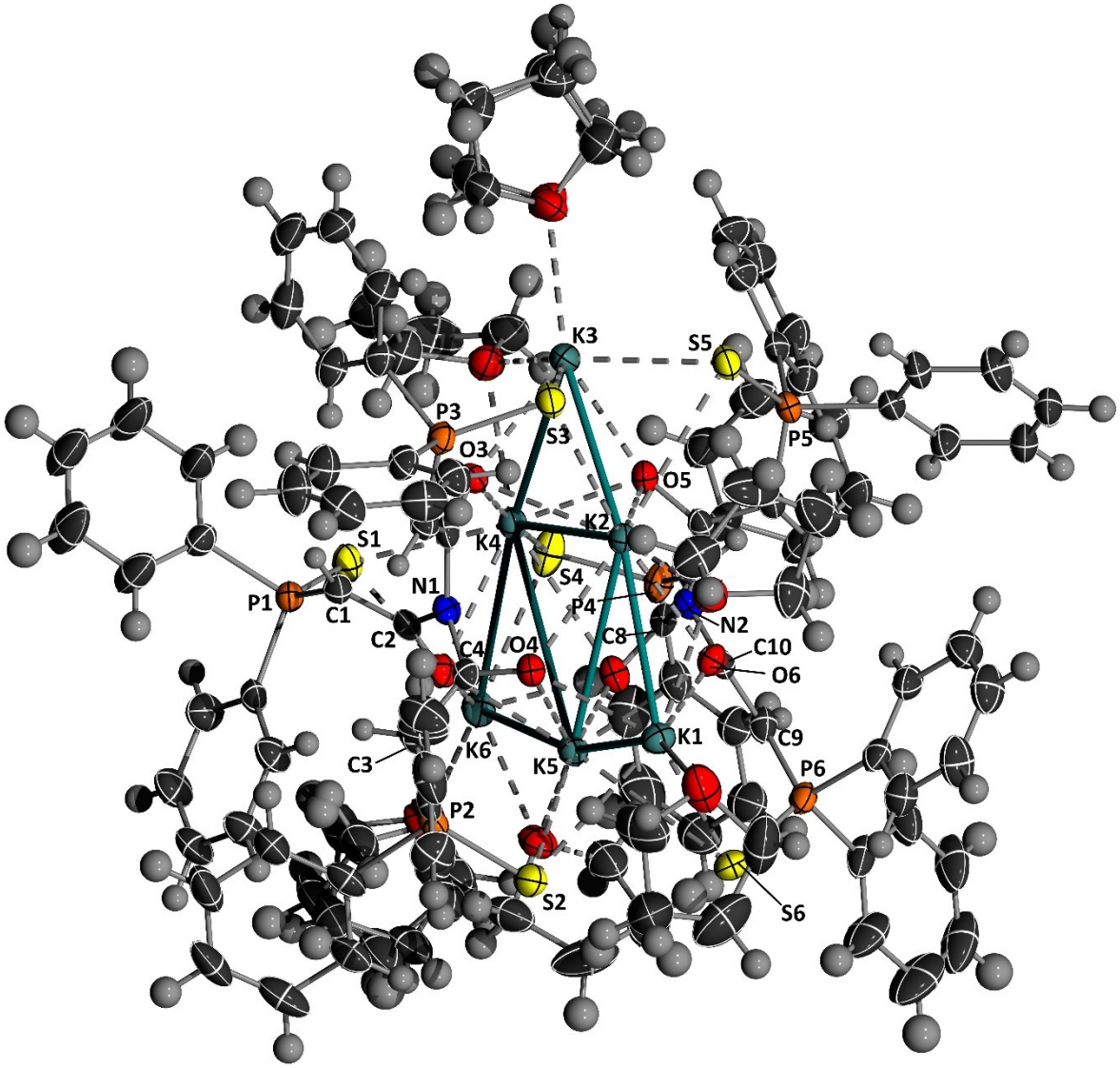

Figure S22. Molecular structure of compound $\mathbf{3^{PS}}$. Thermal ellipsoids at 50% probability level. Selected bond lengths [Å] and angles [°]: C1-C2 1.369(6), C3-C4 1.380(6), C5-C6 1.378(6), N1-C2 1.438(6), N1-C4 1.431(6), N1-C6 1.437(6), C2-O1 1.270(5), C4-O2 1.277(6), C6-O3 1.277(5), P1-C1 1.748(5), P2-C3 1.742(5), P3-C5 1.750(5), P1-S1 1.985(2), P2-S2 1.985(2), P3-S3 1.984(2), P1-C1-C2 121.0(3), P2-C3-C4 123.2(4), P3-C5-C6 122.9(4), C2-N1-C4 119.1(3), C4-N1-C6 119.3(3), C6-N1-C2 119.6(4), C7-C8 1.380(6), C9-C10 1.401(6), C11-C12 1.390(6), N2-C8 1.442(6), N2-C10 1.430(6), N2-C12 1.439(6), C8-O4 1.263(6), C10-O6 1.276(5), C12-O5 1.266(6), P4-C7 1.736(5), P6-C9 1.729(5), P5-C11 1.741(5), P4-S4 1.988(2), P6-S6 1.985(2),, P5-S5 1.982(2),, P4-C7-C8 120.2(4), P6-C9-C10 118.7(4), P5-C11-C12 118.9(3), C8-N2-C10 120.3(34), C10-N2-C12 119.2(3), C8-N2-C12 117.7(4).

4.3. Molecular structure of 3^{PSe}

All hydrogen atoms were placed on ideal positions. The crystal structure contained four disordered THF molecules. The disorders were modelled using SAME, SIMU, and DELU restraints and refined using the PART instructions and free variables, which were optimized to occupancies of 76% and 24%; 35% and 65%; 43% and 57%; 23% and 77%.

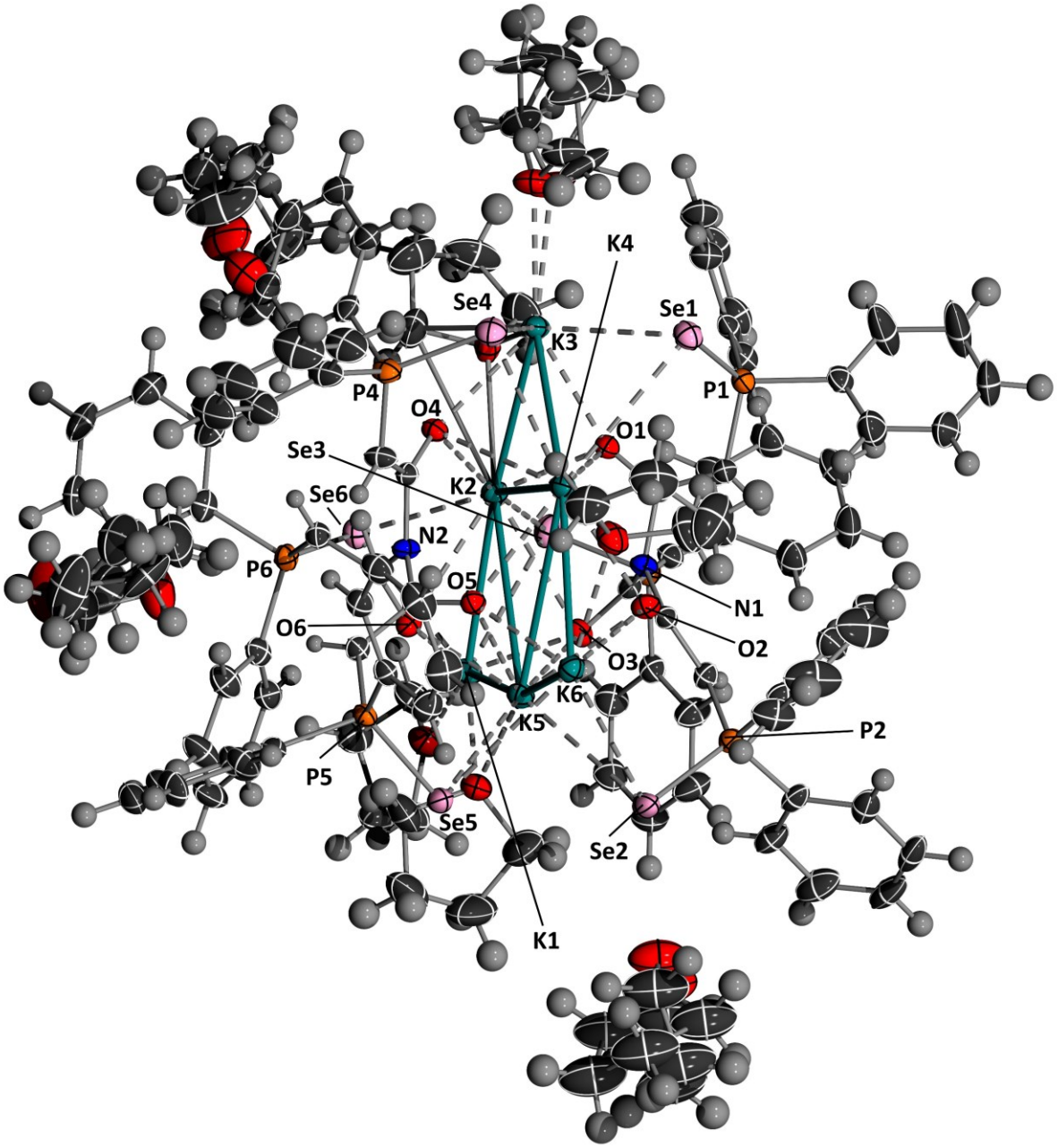

Figure S23. Molecular structure of compound $\mathbf{3^{PSe}}$. Thermal ellipsoids at 50% probability level. Selected bond lengths [Å] and angles [°]: C1-C2 1.379(6), C3-C4 1.379(6), C5-C6 1.384(6), N1-C2 1.442(6), N1-C4 1.437(6), N1-C6 1.440(6), C2-O1 1.259(5), C4-O2 1.266(5), C6-O3 1.265(5), P1-C1 1.743(5), P2-C3 1.736(5), P3-C5 1.739(5), P1-Se1 2.144(1), P2-Se2 2.150(1), P3-Se3 2.140(1), P1-C1-C2 119.3(3), P2-C3-C4 119.0(3), P3-C5-C6 119.2(3), C2-N1-C4 119.6(3), C4-N1-C6 119.9(3), C6-N1-C2 117.5(3), C7-C8 1.376(6), C9-C10 1.372(6), C11-C12 1.383(6), N2-C8 1.438(5), N2-C10 1.435(6), N2-C12 1.445(6), C8-O4 1.265(5), C10-O5 1.264(5), C12-O6 1.264(5), P4-C7 1.741(5), P5-C9 1.740(5), P6-C11 1.740(5), P4-Se4 2.145(1), P5-Se5 2.145(1), P6-Se6 2.148(1), P4-C7-C8 121.9(4), P5-C9-C10 120.0(3), P6-C11-C12 118.9(4), C8-N2-C10 116.6(3), C10-N2-C12 117.7(3), C8-N2-C12 121.2(4).

4.4. Molecular structure of 4^{PS}

All hydrogen atoms were placed on ideal positions.

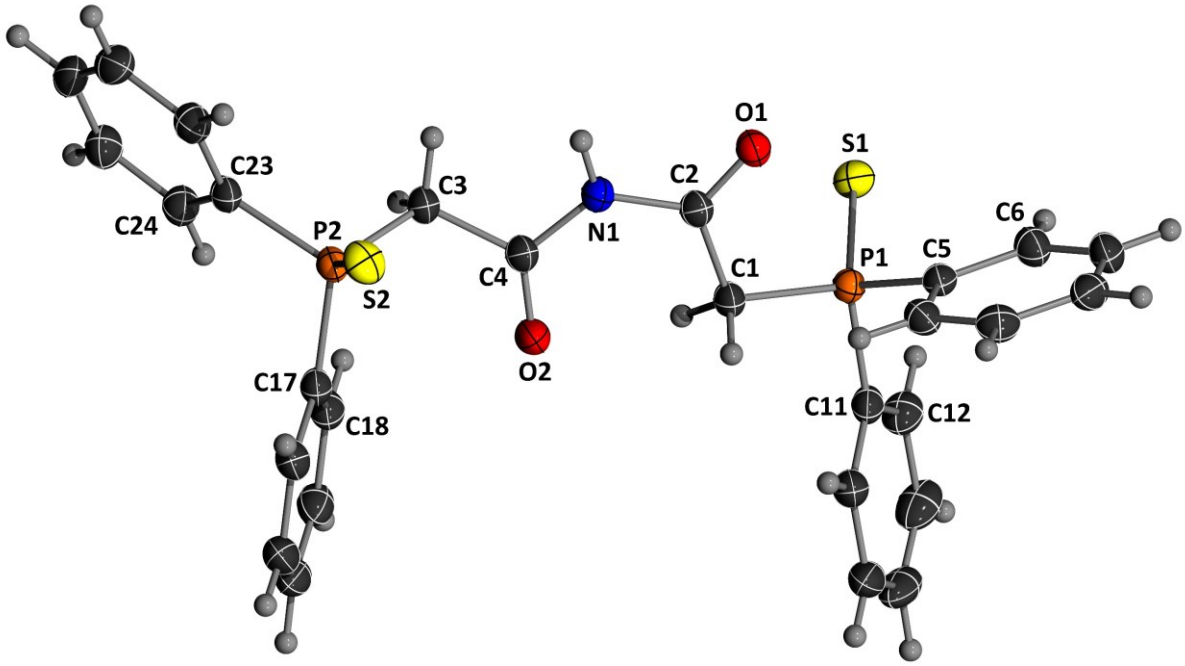

Figure S24. Molecular structure of compound 4^{PSe}. Thermal ellipsoids at 50% probability level. Selected bond lengths [Å] and angles [°]: C1-C2 1.509(2), P1-C1 1.826(2), N1-C2 1.390(2), P1-S1 1.961(1), C1-O1 1.216(2), P1-C1-C2 112.8(1), N1-C2-C1 118.7(1), C3-C4 1.512(2), P2-C3 1.828(2), N1-C4 1.384(2), P2-S2 1.950(1), C4-O2 1.211(2), P2-C3-C4 115.4(1), N1-C4-C3 114.3(1).

5. References

1. M. Jörges, F. Krischer and V. H. Gessner, *Science* 2022, **378,** 1331−1336.
2. F. Krischer, V. S. S. N Swamy, K.-S Feichtner, R. J. Ward and V. H. Gessner, *Angew. Chem. Int. Ed.* 2024, **63**, e202403766.
3. F. Krischer, M. Jörges, T.-F. Leung, H. Darmandeh and V. H. Gessner, *Angew. Chem. Int. Ed.* 2023, 62, e202309629.
4. M. Jörges, S. Mondal, M. Kumar, P. Duari, F. Krischer, J. Löffler and V. H. Gessner, *Organometallics* 2024, **43**, 585−593.
5. G. M. Sheldrick, *Acta Cryst. C,* 2015, **71**, 3–8.
6. G. M. Sheldrick, “SHELXT *Acta Cryst. A* 2015, **71**, 3–8.
7. G. M. Sheldrick, *Acta. Cryst. A* 2007, **64**, 112–122.
8. A. Thorn, B. Dittrich, G. M. Sheldrick, *Acta. Cryst. A* 2012, **68**, 448–451